
HYPEROCTANT SEARCH CLUSTERING: A METHOD FOR CLUSTERING DATA IN HIGH-DIMENSIONAL HYPERSPHERES

Mauricio Toledo-Acosta
Departamento de Matemáticas
Universidad de Sonora (UNISON)
Hermosillo, Son. 83000
mauricio.toledo@unison.mx

Luis Ángel Ramos García
Departamento de Ciencias Computacionales e Inteligencia Artificial
Universidad Autónoma del Estado de Morelos (UAEM)
Cuernavaca, Mor. 62209
luis.ramosgar@uaem.edu.mx

Jorge Hermosillo Valadez*
Departamento de Ciencias Computacionales e Inteligencia Artificial
Universidad Autónoma del Estado de Morelos (UAEM)
Cuernavaca, Mor. 62209
jhermosillo@uaem.mx

March 12, 2025

ABSTRACT

Clustering of high-dimensional data sets is a growing need in artificial intelligence, machine learning and pattern recognition. In this paper, we propose a new clustering method based on a combinatorial-topological approach applied to regions of space defined by signs of coordinates (hyperoctants). In high-dimensional spaces, this approach often reduces the size of the dataset while preserving sufficient topological features. According to a density criterion, the method builds clusters of data points based on the partitioning of a graph, whose vertices represent hyperoctants, and whose edges connect neighboring hyperoctants under the Levenshtein distance.

We call this method *HyperOctant Search Clustering*. We prove some mathematical properties of the method. In order to assess its performance, we choose the application of topic detection, which is an important task in text mining. Our results suggest that our method is more stable under variations of the main hyperparameter, and remarkably, it is not only a clustering method, but also a tool to explore the dataset from a topological perspective, as it directly provides information about the number of hyperoctants where there are data points. We also discuss the possible connections between our clustering method and other research fields.

Keywords High-dimensional clustering · Density · Hyperoctants · Graph Search · Space Transformation.

*Corresponding author.

1 Introduction

Clustering is part of the exploratory data methods that aim at enhancing the practitioner’s natural ability to recognize patterns in the data being studied. Clustering allows to discover underlying structure, to gain insight into data, generate hypotheses, detect anomalies, and identify salient features. Also, it allows to perform natural classification, for instance, to identify the degree of similarity among forms or organisms (phylogenetic relationship); and to investigate compression methods for organizing the data and summarizing it through cluster prototypes.

Cluster analysis of high-dimensional representations of unstructured data is a growing need in the context of artificial intelligence, machine learning and pattern recognition. In this paper, we propose a new clustering algorithm for points in high dimensional spaces endowed with the angular metric. This method is based on a combinatorial-topological approach applied to regions of space defined by signs of coordinates (hyperoctants), the method searches for clusters in a graph encoding the location of groups of points according to their coordinate signs.

In the literature of Machine Learning, we can find many clustering approaches, which we can categorize essentially into two classes: partition-based methods, and hierarchical methods. Our method is an original combination of both. On the one hand, our method is density based, grouping hyperoctants together if they satisfy a condition regarding the density of the possible cluster. Therefore, our method is related to approaches such as DBSCAN [1] and OPTICS [2]. On the other hand, the proposed method builds and partitions a graph. Contrary to state-of-the-art hierarchical methods based on minimum spanning tree or dendograms [3],[4], we construct a connected graph that follows the topology of the hyperoctants of the data space according to the Levenshtein distance. As Levenshtein distance is correlated to cosine similarity, we can work in non-euclidean and discrete spaces (e.g. binary or categorical feature spaces). We call our method HyperOctant Search Clustering (HOS-Clustering).

In high dimensional settings, points lying in a same hyperoctant are close to each other and two neighboring hyperoctants may have close points. We formally prove this assertion. In contrast to current approaches based on graphs, where nodes represent data items, and weighted edges represent similarities among the data items, each node in our graph represents a hyperoctant, connected to neighboring hyperoctants that change by only one dimension. Hence, points lying on neighboring nodes in the graph, imply the closeness of these points in the feature space.

Although classical hierarchical clustering allows for multiple granularity or to automatically discover nested structures [5], our work allows to view data from a different perspective, as it allows for a topological exploration of data points based on overall scales, since the method allows to analyze the topology of the points from two global scales: (1) at the hyperoctant level, and (2) at the level of groups of hyperoctants. As the dimension grows, these global scales are adequate to account for the distribution of the data.

Thus, the proposed method extends the current possibilities of exploring high-dimensional data from a topological perspective. As the method is best suited for high-dimensional data sets containing positive and negative features, typical examples of which are dense vector representations produced by neural networks, the proposed method allows gaining insight into embedded representations of data.

Clustering has many useful applications, in this paper we selected a particular one in order to assess the performance of the proposed method. We tested our method in the task of topic detection. While there have been a significant number of innovative clustering methods in the field of image processing, whether for image segmentation [6], or clustering purposes [7], novel text clustering methods beyond k-means [8, 9, 10] are still missing. Over the last two decades, breakthrough neural network language models [11, 12, 13, 14, 15, 16] have enabled the derivation of embedded vector representations of text units of different kinds, which capture various syntactic and semantic properties of written language [17]. Interestingly, the purpose of the semantic spaces generated by these models bear a remarkable resemblance to theories on neural coding [18]. Moreover, these kind of embeddings have attracted the attention of other scientific disciplines, not only to investigate semantic phenomena related to language [19], but also, for example, to represent genetic code [20]. Thus, there is indeed a huge potential in the discovery of new methods that allow to explore this type of computational representations more effectively. Given that our method is a density-based clustering method, we compare its results to those produced by DBSCAN as baseline. The comparison was done in three different text corpora.

The rest of this paper is organized as follows: In Section 2, we situate our contribution with respect to related work. In Section 3, we formally describe the clustering method, and the experimental design to assess its performance. In Section 4, we present the experimental results, that we discuss in Section 5. We conclude the paper in Section 6 where we summarize our contributions.

2 Related work

Clustering methods can be categorized into three classes: Hierarchical, Partitioning and Density based. Hierarchical techniques produce a nested sequence of partitions, with a single, all-inclusive cluster at the top and singleton clusters of individual points at the bottom. Depending on whether an ascending or descending process is followed, the clustering is either “agglomerative” or “divisive” [21]. Partitioning algorithms can be better understood from the notion of distance and neighbor. The best known algorithms in this class are *K-means* [22], with its variants such as Spherical K-Means [23], Multi-Cluster Spherical K-Means [24] or Robust and Sparse K-Means [25], and *K-nearest-neighbors* [26]. Both approaches have been widely reported in the literature, with an emphasis on improving computational performance and reducing complexity [27, 28, 29]. Density based clustering aims at finding clusters at different levels of granularity with appropriate noise filtering, depending on the notion of density of a region [30]. Over the last two decades, numerous density based clustering techniques have been proposed (for example, see [31] for a recent review).

For clustering purposes, the most relevant aspect of the curse of dimensionality concerns its effect on distance or similarity: a finite set of data points becomes increasingly “sparse” as the dimensionality increases, thus distances between points become relatively uniform [32]. Hence, meaningful clusters are harder to detect as distances are increasingly similar for growing dimensionality.

One approach to deal with this phenomenon is to reduce the dimensionality of the data. Some techniques for clustering high dimensional data have included both feature transformation and feature selection techniques. Feature transformation algorithms employ dimensionality reduction to project data into a lower dimensional meaningful space, thus uncovering latent structure in data [33]. In this category, we can include the learning to hash or binary code learning methods [34, 35, 36, 37]. Recently, binary encoding has been combined with classical approaches to clustering, such as k-means [38], or k-nearest-neighbors [39]. Feature selection methods select only the most relevant of the dimensions to reveal groups of objects that are similar on only a subset of their attributes. Subspace clustering [40, 41, 42, 43] is an extension of feature selection that attempts to find clusters in different subspaces of the same data set [44].

When working with embedded representations, searching for clusters in the full feature set is important, as it has been empirically shown that these representations cluster by semantic similarity (topic similarity), which is a property captured by the full vector. Hence, the search for clusters in the whole set of features is key, and thus feature selection or feature transformation methods are often not adequate for clustering text entities. In this case, density-based methods such as DBSCAN are more effective. However, hyper-parameter tuning is not a trivial task when dealing with high-dimensional data, and therefore, the correct use of these methods is challenging [45, 46].

It has been recognized that the similarity measure is a key factor for clustering. However, it is still challenging for existing similarity measures to cluster non-spherical data with high noise levels [47]. From a theoretical point of view, the way we use Levenshtein distance is isomorphic to the Hamming distance, as our $\{+, -\}^D$ labels are isomorphic to $\{0, 1\}^D$ strings. The relevance of Hamming distance in the context of pattern recognition has been subject of theoretical analysis in the past [48]. Furthermore, it has been shown that for very small distances, it is possible to demonstrate the equivalence of distance measures, commonly employed in the context of clustering (e.g. hamming distance), in order to compare partitions created by different methods [49].

Furthermore, it has been shown that most clustering tasks are NP-hard [50], and that for a set of three simple properties: scale invariance; richness, the requirement that all partitions are realisable; and a consistency condition on the reduction and stretching of individual distances, there is no clustering function that satisfies all three [51]. This indicates that basic trade-offs are inherent to any solution of a clustering problem.

In these regards, we provide evidence that our method is a sound alternative to perform clustering tasks in high-dimensional spaces endowed with the angular metric, with the additional advantages that it allows to acquire insight about some topological properties of the semantic space, and also, its performance is more stable under variations of its most important hyperparameter.

3 Methods

HOS-Clustering is a density-based clustering algorithm. The method regards clusters as high density regions separated by neighborhoods of low density. The search for these regions is performed in terms of the location of the hyperoctants containing points of the data set; that is, we consider the signs of the coordinates of each point. As a consequence of this loosely constrained approach, clusters found by HOS-Clustering do not have special geometric restrictions, such as convexity in other clustering methods. Our method assumes that the underlying metric in the data set space is the angular metric, or equivalently, the cosine similarity.

We start with the necessary definitions and background. Then we detail our clustering method together with the tools we use to assess its performance in topic detection tasks.

3.1 Notation and Background

Consider the metric space $(\mathbb{R}^D \setminus \{0\}, d)$, where $d : [-1, 1] \rightarrow [0, \pi]$ is the angular metric given by

$$d(u, v) = \arccos \left(\frac{u \cdot v}{|u| \cdot |v|} \right).$$

Here, $u \cdot v$ denotes the dot product in \mathbb{R}^D , and \mathbf{z} denotes the Euclidean norm of $z \in \mathbb{R}^D$. Since $d(r_1 u, r_2 v) = d(u, v)$ for any $r_1, r_2 > 0$, we only consider points lying in the unit sphere $\mathbb{S}^{D-1} \subset \mathbb{R}^D$. Recall the cosine similarity given by

$$\text{sim}(u, v) = \frac{u \cdot v}{|u| \cdot |v|}.$$

The *diameter* of a finite set $B \subset \mathbb{R}^D$ is defined as

$$\text{diam}(B) = \max\{d(x, y) \mid x, y \in B\}.$$

Let the *linear density* (or density) of a finite set $B \subset \mathbb{R}^D$, $\mathbf{B} > 1$, be:

$$\delta(B) = \frac{|B|}{\text{diam}(B)}, \tag{1}$$

where \mathbf{B} denotes the number of elements of B . This function δ accounts for the density of the set B , in terms of how many elements it contains with respect to the maximum distance between the elements. Typically, the density is measured in terms of elements per D -dimensional units of volume. However, in order to avoid dealing with the term $\text{diam}(B)^D$ which can be very small, or very large, as the dimensionality D increases, we consider instead the linear density given by Equation (1).

3.1.1 Hyperoctants

Hypercotants as strings of signs. We consider the space $\mathbb{R}^D \setminus \{0\}$ divided into 2^D pairwise disjoint open regions, called hyperoctants. A hyperoctant is a region of space defined by one of the 2^D possible combinations of coordinate signs (\pm, \dots, \pm) . For example, in \mathbb{R}^3 , the combinations $+++$ and $-+-$ determine the following hyperoctants

$$\begin{aligned} +++ &: \{(x_1, x_2, x_3) \in \mathbb{R}^3 \mid x_1, x_2, x_3 > 0\} \\ -+- &: \{(x_1, x_2, x_3) \in \mathbb{R}^3 \mid x_1, x_3 < 0, x_2 > 0\} \end{aligned} \tag{2}$$

Observe that points with some coordinate equal to 0 are not contained in any hyperoctant according to this definition. However, we do not expect this to be a problem since 0-valued coordinates in the embeddings produced by neural networks are very unusual.

In low dimensional cases there are only a few hyperoctants (for example, there are only 4 quadrants in \mathbb{R}^2). However, as the dimension D increases, the number of hyperoctants increases exponentially. In this case, the size of any finite set of points \mathbf{A} becomes much smaller than the number of hyperoctants. This means that the string of signs defining the hyperoctant of each point is a useful label for its location in space. At the same time, as D increases, whenever two points are in the same hyperoctant, it means that they are close to each other, and probably have to be in the same cluster. This observation is formalized as follows.

Observation 1. Let S_D be the surface area of \mathbb{S}^{D-1} . We denote by S_D^{HO} the surface area of the intersection of each hyperoctant and \mathbb{S}^{D-1} . Since there are 2^D hyperoctants, S_D^{HO} is given by

$$S_D^{\text{HO}} = \frac{S_D}{2^D} = \begin{cases} \frac{\pi^k (k-1)!}{(2k-1)!}, & \text{if } D = 2k, \text{ for some integer } k \\ \frac{\pi^{k+1}}{4^k k!}, & \text{if } D = 2k + 1, \text{ for some integer } k. \end{cases}$$

It is straightforward to verify that $\lim_{D \rightarrow \infty} S_D^{\text{HO}} = 0$. This means that, as the dimension D increases, the region of space determined by each hyperoctant gets smaller with respect to the total area of S^{D-1} . Therefore, as D increases, the fact that two points lie in the same hyperoctant means that they are close to each other.

Distance between hyperoctants. We will denote each hyperoctant by its respective “*sign label*” as we did in the example described in (2). In this regard, a sign label is an element of $\{+, -\}^D$; that is, a string of size D over the alphabet $\{+, -\}$. To determine the proximity of two hyperoctants, in a way that reflects the angular distance between the points located at these hyperoctants, we use the Levenshtein distance d_L between their sign labels [52]. This distance is defined as the number of places where the two strings are different. For example, in \mathbb{R}^3 ,

$$d_L(+ + +, - + -) = 2.$$

In the sequel, we will refer to a sign label by the symbol ϕ . It is worth noting that the sign label ϕ defining the hyperoctant containing some point $v \in \mathbb{R}^D$ is directly related to the sign vector of $v = (v^{(1)}, \dots, v^{(D)})$, defined as $\sigma_v = (\sigma_v^{(1)}, \dots, \sigma_v^{(D)})$ where

$$\sigma_v^{(k)} = \begin{cases} 1, & v^{(k)} \geq 0 \\ -1, & v^{(k)} < 0. \end{cases}$$

Alternatively, the sign vector is given by

$$\sigma_v = \left(\frac{v^{(1)}}{|v^{(1)}|}, \dots, \frac{v^{(D)}}{|v^{(D)}|} \right).$$

We will denote the one-to-one correspondence between a sign vector and its sign label by writing: $\sigma \sim \phi$. Thus, we use indistinctly the sign vector, or sign label, to compute Levenshtein distances between hyperoctants, and sign labels for identifying each hyperoctant during the clustering process.

For any point $v \in \mathbb{R}^D$, we denote by $h : \mathbb{R}^D \rightarrow \{+, -\}^D$ the function mapping v to the the sign label defining the hyperoctant containing v . Thus we have:

$$\begin{array}{ccc} v \in \mathbb{R}^D & \xrightarrow{\sigma} & \sigma_v \in \mathbb{R}^D \\ & \searrow h & \swarrow \sim \\ & h_v \in \{+, -\}^D & \end{array}$$

For example, if $v = (-3, 2)$, then $\sigma_v = (-1, 1)$, and the sign label is given by $h_v = -+$.

If we consider two points $u, v \in \mathbb{R}^D$, we can define the Levenshtein distance between them by

$$d_L(u, v) := d_L(h_u, h_v).$$

Now, we describe a way to compute all Levenshtein distances between all pairs of row vectors in a matrix. Let A be a matrix of N row vectors $A \in \mathcal{M}_{N \times D}(\mathbb{R})$ given by

$$A = \begin{pmatrix} v_1 \\ \dots \\ v_N \end{pmatrix}.$$

The Levenshtein distance d_L between two row vectors $v = (v^{(1)}, \dots, v^{(D)})$ and $w = (w^{(1)}, \dots, w^{(D)})$ can be computed as follows

$$d_L(v, w) = \frac{D - \sum_{i=1}^D \frac{v^{(i)} w^{(1)}}{|v^{(i)}| |w^{(i)}|}}{2}. \quad (3)$$

We denote by A_σ the matrix consisting of the sign row vectors. Using Equation (3), we can define a matrix Δ_L , whose entry i, j is the Levenshtein distance $d_L(v_i, v_j)$, as follows

$$\Delta_L = \frac{1}{2} (\mathbf{D} - A_\sigma \cdot A_\sigma^T),$$

where $\mathbf{D} \in \mathcal{M}_{N \times N}(\mathbb{N})$ is the matrix with every entry equal to D .

Evidence suggests that there is a correlation between the angular distance between pairs of points, and the Levenshtein distance between their respective hyperoctant sign labels (see Figures 1a and 1c). This is also supported by the fact that $d_L(\sigma_u, \sigma_v) + u \cdot v \leq D$. Because of this, one can replace the notion of *closeness* using the angular distance between points with the Levenshtein distance between their respective sign labels. In Section 3.1.2 we will analyze the details of this substitution.

On the other hand, there is a weaker correlation between the Euclidean distance and the Levenshtein distance (see Figures 1b and 1d). All four sub-figures in Figure 1 correspond to two particular data sets of word embeddings, which have been included here without further details for illustrative purposes.

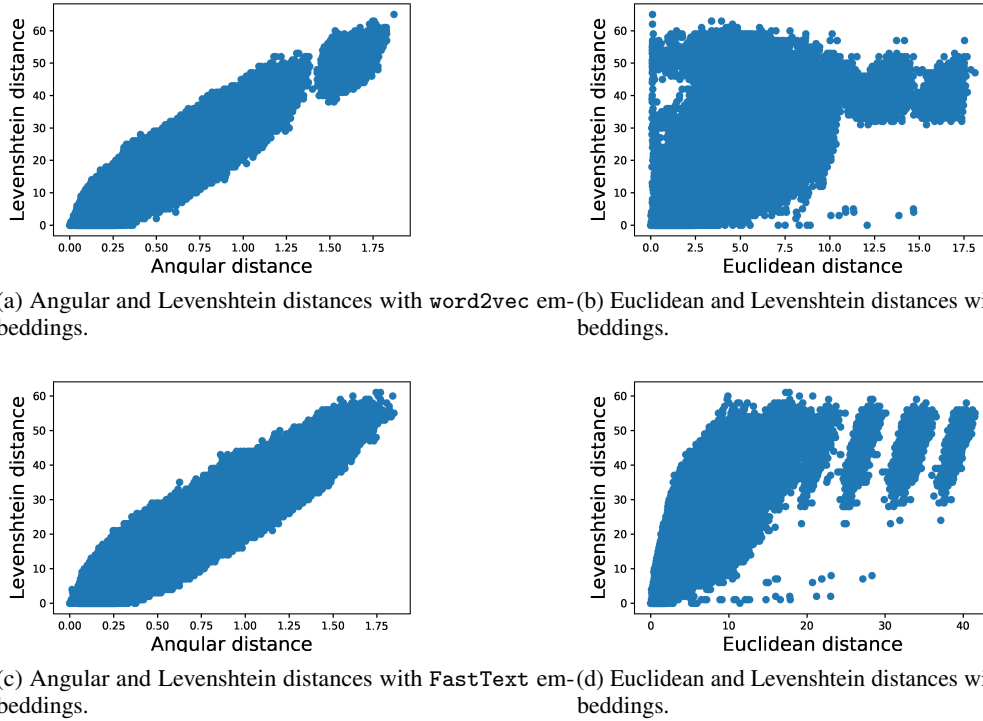


Figure 1: The Levenshtein distance can be a good substitute for the angular distance (left), but not so much for the Euclidean distance (right). In both cases data points correspond to either word2vec [53] or FastText [54] embeddings.

Encoding hyperoctants' proximity using graphs. The set of hyperoctants of a D -dimensional space has a combinatorial structure which encodes the location of each hyperoctant with respect to the others. We can encode this information in the following graph $P_D = (V, E)$. The set V is the set of hyperoctants labeled by their respective sign label ϕ . Two sign labels ϕ_1 and ϕ_2 are connected by an edge in E if the Levenshtein distance between ϕ_1 and ϕ_2 is 1. In Figure 2 we show an example of the graph P_D for $D = 3$.

As the number of nodes and edges of P_D increases exponentially with D , we restrict our attention to a *smaller* graph. Let $A \subset \mathbb{R}^D$ be a finite set, we will define a weighted graph $G_0 = (V_0, E_0)$ as follows:

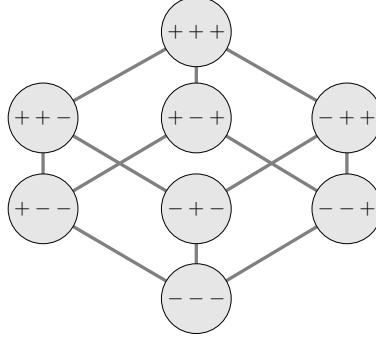


Figure 2: The graph P_D for $D = 3$ representing the spatial location of the 8 octants of \mathbb{R}^3 .

- The set V_0 is the set of sign labels, defining the hyperoctants containing points of A . That is

$$V_0 = \{h_v \mid v \in A\}.$$

- Two sign labels ϕ_1 and ϕ_2 are connected by an edge in E_0 if, either $\overline{\phi_1\phi_2} \in E$ or the following condition holds: any minimal length path between ϕ_1 and ϕ_2 in P_D contains no elements of V_0 . The weight associated to the edge is $d_L(\phi_1, \phi_2)$.

We call the graph G_0 , the *reduced graph* of A . In Figure 3, we show an example of the construction of this graph. We start with the 8 octants of \mathbb{R}^3 , given by their respective signs, represented in the graph P_D . The set $V_0 = \{+--, ++-, --+, +++\}$ is depicted in red, both as a set of nodes of P_D (Figure 3a), and as a set of nodes of G_0 (Figure 3b).

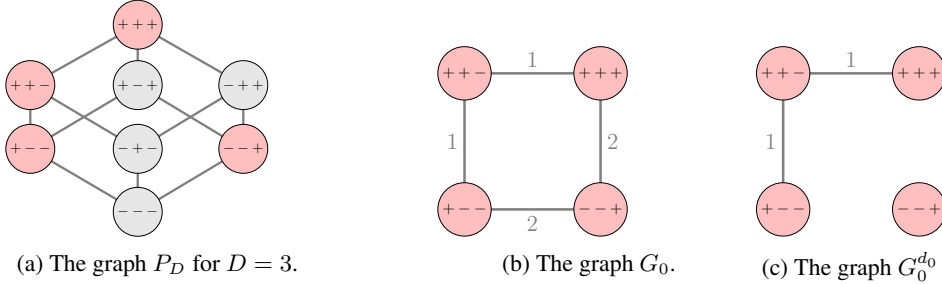


Figure 3: Construction of the graphs G_0 and $G_0^{d_0}$, the graph obtained by deleting the edges of G_0 such that $d_L(\phi_1, \phi_2) > d_0$. Elements of V_0 (that is, hyperoctants containing data points) are colored in red.

We have the following propositions, the first of which is straight-forward to verify.

Proposition 1. Any minimal length path in P_D between v and w has length $d_L(v, w)$.

Proposition 2. The graph G_0 is connected.

Proof: Let $\phi, \psi \in V_0$ be two sign labels. If $\overline{\phi\psi} \in E$, then $\overline{\phi\psi} \in E_0$. If $\overline{\phi\psi} \notin E$, we have two cases:

- Any minimal length path between ϕ and ψ in P_D contains no elements of V_0 . It follows that $\overline{\phi\psi} \in E_0$.
- There exists a minimal length path between ϕ and ψ in P_D containing an element $y \in V_0$. In this case, let \mathcal{P} be the collection of such minimal length paths. For the sake of clarity, we will consider that any path $q \in \mathcal{P}$ is a collection of nodes that we denote

$$q = \{\phi = y_0, y_1, \dots, y_{k-1}, y_k = \psi\}.$$

Let $q \in \mathcal{P}$ be such that $|V_0 \cap q| \geq |V_0 \cap p|$ for any $p \in \mathcal{P}$. We now show that $\overline{y_0y_1}, \dots, \overline{y_{k-1}y_k} \in E_0$. Let us assume that y_j and y_{j+1} are not connected by an edge in E_0 , then there exists a minimal length path in P_D

between y_j and y_{j+1} containing an element $x \in V_0$. Therefore, the path

$$q' = \{\phi = y_0, y_1, \dots, y_j, x, y_{j+1}, \dots, y_{k-1}, y_k = \psi\}$$

has length $d_L(\phi, \psi)$, and $q \subset q'$ contradicting that q is maximal. Therefore,

$$\overline{y_0 y_1}, \dots, \overline{y_{k-1} y_k} \in E_0$$

and thus, there is a path in G_0 between ϕ and ψ . This shows that G_0 is connected.

This proposition means that the graph G_0 on which we will perform our search is always connected and, therefore, all points are *reachable* by some walk. This situation is desirable if we want to consider all points in a data set in the clustering process.

However, if the data set contains highly isolated points, and given that the graph G_0 is connected, these isolated points will be connected to their nearest neighbours, no matter how far they are. This, in turn, might introduce noise to the clustering algorithm. This behaviour can be compensated by imposing a maximum distance threshold d_0 on the graph G_0 , thus disconnecting the points that are too far apart and discarding them from the clustering process. We denote by $G_0^{d_0}$ the graph G_0 obtained by deleting the edges of G_0 whose weight is greater than d_0 . By appropriately choosing d_0 , the hyperoctants containing points far apart are disjointed nodes in this new graph $G_0^{d_0}$.

Observe that $G_0 = G_0^D$. Therefore, we will use the graph $G_0^{d_0}$, with d_0 being a hyperparameter depending on the nature of the data set. Typically, we choose d_0 greater than the average edge weight in G_0 . Figure 3c shows an example of $G_0^{d_0}$.

3.1.2 Centering Value for the data set

Now, we turn our attention to the question of whether the sign label of each hyperoctant adequately represents the points in the hyperoctant. In order to increase the effectiveness of the algorithm by replacing the notion of proximity between points, using the angular metric, by the notion of the Levenshtein distance between hyperoctant labels, it is desirable that as many points in the data set as possible are *centred* within their respective hyperoctants. To illustrate this, note Figure 4a, where it can be seen that points v_1 and v_2 are more likely to belong to the same cluster, but the points are not *optimally* centered on their respective hyperoctants. After applying an adequate rotation R around the origin, Figure 4b shows that the same points are now located closer to the center of their respective hyperoctants.

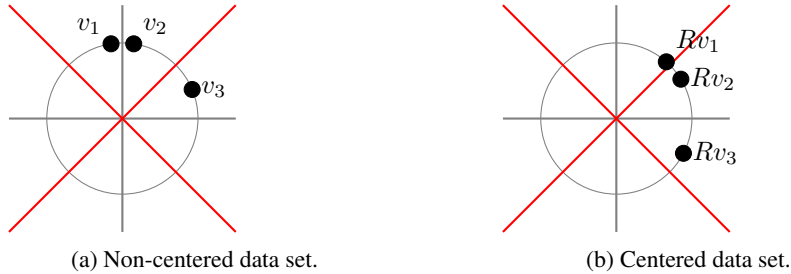


Figure 4: The same set of points under different coordinates.

This notion can be quantified by measuring, via the cosine similarity, how close each point v is to the middle point of its respective hyperoctant. Given an hyperoctant defined by its sign label ϕ , we say that its middle point is a point σ_v such that $\sigma_v \sim \phi$.

$$\text{sim}(v, \sigma_v) = \frac{1}{\sqrt{D}} \sum_{j=1}^D |v^{(j)}|.$$

Given a finite set $A = \{v_1, \dots, v_N\} \subset \mathbb{S}^{D-1} \subset \mathbb{R}^D$, with $v_i = (v_i^{(1)}, \dots, v_i^{(D)})$, the average similarity between elements of A and the respective middle point of their hyperoctant is given by

$$\mathbf{c}(A) = \frac{1}{N} \sum_{k=1}^N \text{sim}(v_k, \sigma_{v_k}) = \frac{1}{N\sqrt{D}} \sum_{k=1}^N \sum_{j=1}^D |v_k^{(j)}|.$$

We call $\mathbf{c}(A)$ the *centering value* of a finite set $A \subset \mathbb{S}^{D-1}$, and we use it as a measure quantifying the average centering of the elements of A . In Figure 4, the set of points in 4a has a lower centering value than the set of points in 4b.

3.1.3 Rotations in \mathbb{R}^D

A rotation is a distance-preserving transformation of a D -dimensional Euclidean space. Equivalently, a rotation can be regarded as a $D \times D$ orthogonal matrix. Observe that a rotation is also a symmetry of the unit sphere \mathbb{S}^{D-1} endowed with the angular metric. Up to a change of basis, a rotation is given by a matrix

$$R_{\Theta} = \begin{pmatrix} R_{\theta_1} & & & & \\ & \ddots & & & \\ & & R_{\theta_k} & & \mathbf{0} \\ & & & 1 & \\ \mathbf{0} & & & & \ddots \\ & & & & & 1 \end{pmatrix},$$

where $\Theta = \{\theta_1, \dots, \theta_k\}$ is a collection of k angles $\theta \in [0, 2\pi)$, and R_{θ} is a 2-dimensional rotation matrix with angle θ . Observe that $k \leq \lfloor \frac{D}{2} \rfloor$. In general, a rotation matrix is given by

$$R_{\Pi, \Theta} = PR_{\Theta}P,$$

where Π is a set of k pairs (i, j) , each of these indicating which coordinates are rotated with the respective angle θ . The matrices P are permutation matrices determining the change of coordinates.

For example, the 5-dimensional rotation matrix $R_{\Pi, \Theta}$ with $\Pi = \{(1, 3), (2, 5)\}$ and $\Theta = \{\frac{\pi}{4}, \frac{\pi}{6}\}$ is explicitly given by

$$R_{\Pi, \Theta} = \begin{pmatrix} \cos \frac{\pi}{4} & 0 & -\sin \frac{\pi}{4} & 0 & 0 \\ 0 & \cos \frac{\pi}{6} & 0 & 0 & -\sin \frac{\pi}{6} \\ \sin \frac{\pi}{4} & 0 & \cos \frac{\pi}{4} & 0 & 0 \\ 0 & 0 & 0 & 1 & 0 \\ 0 & \sin \frac{\pi}{6} & 0 & 0 & \cos \frac{\pi}{6} \end{pmatrix}.$$

Given a finite set of points A , we seek a rotation matrix $R_{\Pi, \Theta}$ maximizing the value $\mathbf{c}(R_{\Pi, \Theta}A^T)$. This rotation matrix is parameterized by a pair (Π, Θ) given as before. Once we find the adequate rotation matrix, we can replace the set A by $R_{\Pi, \Theta}A^T$ to obtain a better centered set of points in the sense of Figure 4.

3.2 The Clustering Method

Now, we describe the proposed clustering method using the notation and ideas developed in Subsection 3.1.

We start with a D -dimensional data set of size N' , which is a finite set

$$A = \{v_1, \dots, v_{N'}\} \subset \mathbb{S}^{D-1} \subset \mathbb{R}^D.$$

Using an optimization method (for example, local search of global optimum like simulated annealing), we first find a rotation $R_{P, \Theta}$ maximizing the centering value $\mathbf{c}(A)$ of the data set. We replace the set A by $R_{P, \Theta}A^T$, and denote this new set again by A .

We identify each point $v \in A$ by its sign label $h_v \in \{+, -\}^D$, which defines an hyperoctant in \mathbb{R}^D . From the construction of the reduced graph G_0 , recall the set of sign labels

$$V_0 = \{h_v \mid v \in A\}.$$

Since we can have two or more points in a same hyperoctant, it follows that

$$N := |V_0| \leq |A| = N'. \quad (4)$$

It is worth observing that, in practice, the rotation of the data set increments the difference $N' - N$, thus reducing the size of the data set, which improves the performance of the clustering method.

From this point on, two points lying in the same hyperoctant will be considered as the same instance during the clustering process. In other words, at the end of the process, if one point is in a cluster, all other points in the same hyperoctant will be in the same cluster. The motivation behind this principle was given by Observation 1.

The clustering principle starts by identifying hyperoctants containing more than one point. These subsets of points are *potential* clusters (we call them ‘proto-clusters’). Then, we construct $G_0^{d_0}$ and perform a walk through this graph starting from the node with minimal combined Levenshtein distance to every other node. As we walk, we group nodes together according to a density criterion. The result is a collection of subsets of nodes of $G_0^{d_0}$, possibly including some proto-clusters. These subsets together with all proto-clusters not included in the previous collection, will become true clusters if they verify a cardinality condition. Figure 5 depicts the process for a simple data set, where some assumptions are made for illustration purposes.

We now describe the formal details of the process. We denote by $\varphi_0 \in V_0$ the sign label with the minimal combined Levenshtein distance to every other element of V_0 . That is,

$$\varphi_0 = \operatorname{argmin}_{\phi \in V_0} \sum_{\psi \in V_0} d_L(\phi, \psi).$$

We denote by P_ϕ the set of points in A lying in the hyperoctant defined by the sign label ϕ . Formally,

$$P_\phi = \{v \in A \mid \sigma_v \sim \phi\}.$$

As previously stated, the step shown in inequality (4), induces a reduction of the number of entities. At the same time, it forms the first *proto-clusters*, which later might be enriched with new elements. By a *proto-cluster* we mean a set P_ϕ such that $|P_\phi| > 1$, for some $\phi \in V_0$. We keep track of these *proto-clusters* by defining

$$W_0 = \{\phi \in V_0 \mid |P_\phi| > 1\}.$$

Now, we construct the reduced graph $G_0^{d_0}$. The clustering method searches for clusters by walking the reduced graph $G_0^{d_0}$, for some d_0 , using a Breadth First Search (BFS) starting at the node φ_0 . This BFS-walk enumerates the nodes in V_0 as a sequence $\varphi_0, \varphi_1, \dots, \varphi_N$. We group nodes together in sets $C_i \subset V_0$ if the set of points they represent has density greater or equal than a minimum density δ_0 , we call this the *density condition*. We say that a set C satisfies the density condition if

$$\operatorname{diam}(C) \leq \frac{|C|}{\delta_0}. \quad (5)$$

The result is a collection of subsets $C_i \subset V_0$, denoted by \mathcal{C}_0 , where every C_i must also satisfy the condition $|\cup_{\phi \in C_i} P_\phi| \geq k_0$, where k_0 is the minimum number of elements in a cluster. Out of the set of hyperparameters $\{d_0, k_0, \delta_0\}$, δ_0 is actually the most important as it controls the resulting number of clusters. Next, we enrich this collection \mathcal{C}_0 with nodes from W_0 not belonging to any element of \mathcal{C}_0 , and denote this enhanced collection by

$$\mathcal{C}_1 = \mathcal{C}_0 \cup \left\{ \{\varphi\} \mid \begin{array}{l} \varphi \in W_0, \\ \varphi \notin C \text{ for any } C \in \mathcal{C}_0 \end{array} \right\}.$$

Now, we take the subsets of A corresponding to the elements of \mathcal{C}_1 . We define

$$\mathcal{C}_2 = \left\{ \bigcup_{\phi \in C} P_\phi \mid C \in \mathcal{C}_1 \right\}. \quad (6)$$

Observe that \mathcal{C}_2 is a collection of subsets of A . This is the collection of clusters.

As a consequence of the density condition (5), and (6), our method produces a clustering of A which is not a partition. We regard points not belonging to any cluster as *noise*. The clustering method is summarized in Algorithm 1.

To illustrate the clustering method we provide two walk-through examples depicted in Figures (5) and (6). It is worth stressing that the method works best with points in high-dimensional spaces. In low dimensional spaces, the method produces trivial results, except for very specific configurations of points; the examples are presented for illustrative

Algorithm 1 HOS-Clustering

Require: A : data set of points, $A = \{v_1, \dots, v_N\} \subset \mathbb{S}^{D-1} \subset \mathbb{R}^D$, with $v_i = (v_i^{(1)}, \dots, v_i^{(D)})$, k_0 : minimum number of elements in a cluster ($k_0 > 1$), δ_0 : minimum density of every cluster, d_0 : maximum Levenshtein distance between nodes of G_0 .

1: $R_{\Pi, \Theta} \leftarrow \underset{R_{\Pi, \Theta}}{\operatorname{argmax}} \mathbf{c}(R_{\Pi, \Theta} A^T)$ ▷ where $\mathbf{c}(A) = \frac{1}{N\sqrt{D}} \sum_{k=1}^N \sum_{j=1}^D |v_k^{(j)}|$

2: $A \leftarrow R_{\Pi, \Theta} A^T$

3: $V_0 \leftarrow \{h_v \mid v \in A\}$

4: $P_\phi \leftarrow \{v \in A \mid \sigma_v \sim \phi\}$

5: $W_0 \leftarrow \{\phi \in V_0 \mid |P_\phi| > 1\}$

6: $\text{Build}(G_0^{d_0})$

7: $\mathcal{C}_0 \leftarrow \{\}$ ▷ empty collection of subsets of V_0

8: $\varphi_0 \leftarrow \underset{\phi \in V_0}{\operatorname{argmin}} \sum_{\psi \in V_0} d_L(\phi, \psi)$

9: $\mathbf{s} \leftarrow \text{BFS}(G_0^{d_0}, \varphi_0)$ ▷ This search enumerates the nodes in V_0 as a sequence $\mathbf{s} = \varphi_0, \dots, \varphi_N$

10: $i \leftarrow 0, j \leftarrow 0$

11: **while** $j \leq N$ **do**

12: Form the possible cluster $C_i \leftarrow \{\phi_j\}$

13: **while** $\text{diam}(C_i \cup \{\phi_{j+1}\}) \leq \frac{|C_i|+1}{\delta_0}$ **and** $j < N$ **do**

14: add ϕ_{j+1} to C_i

15: $j = j + 1$

16: **end while**

17: **if** $|\cup_{\phi \in C_i} P_\phi| \geq k_0$ **then**

18: add the set C_i to the collection \mathcal{C}_0

19: $i = i + 1$

20: **end if**

21: **end while**

22: $\mathcal{C}_1 \leftarrow \mathcal{C}_0 \cup \left\{ \{\varphi\} \mid \begin{array}{l} \varphi \in W_0, \\ \varphi \notin C \text{ for any } C \in \mathcal{C}_0 \end{array} \right\}$

23: $\mathcal{C}_2 \leftarrow \left\{ \bigcup_{\phi \in C} P_\phi \mid C \in \mathcal{C}_1 \right\}$

Ensure: \mathcal{C}_2

purposes. The first example does not include rotations. The second example shows the effect of a rotation. In this example, if we choose a small enough δ_0 , we could end up with one cluster $C_2 = \{p_1, p_2, p_3\}$. If we choose a large enough δ_0 , we could end up with no clusters.

3.3 Experimental design to evaluate the method

In this section, we describe the implementation of the clustering method as a tool for topic detection. The question we address in this work is how to systematically explore, via clustering, the similarities between text vector representations, in order to discover semantic relationships possibly encoded by patterns of signs in the embeddings.

We also describe the measures that we use for its evaluation, and its comparison with DBSCAN.

We start with a corpus of N documents \mathbf{d}_i , each one with a label indicating the topic of the document denoted by an integer y_i . We will generate D -dimensional embeddings for the documents \mathbf{d}_i using two main approaches:

1. Document embeddings using `doc2vec`.
2. Means of word embeddings using `word2vec`, `FastText` and `GloVe`. We decided not to use transformer embeddings (for example, from BERT: [15]) because that implied designing evaluation measures adapted to the contextual representation of this type of models.

In both approaches, each document \mathbf{d}_i is represented by a point $v_i \in \mathbb{S}^{D-1}$. We apply the clustering method to the set of points $\{v_1, \dots, v_N\}$, yielding a set of clusters $\mathcal{C} = \{C_1, \dots, C_M\}$. We evaluate the quality of these clusters, both in terms of intrinsic coherence of the topic words in each cluster, and in terms of distance to the ground truth clustering. We use the following approaches:

1. Topic Coherence using the cosine similarity [55]. We define the topic coherence as follows. For each cluster $C \in \mathcal{C}$, we denote the set of documents represented by the cluster C by $C^d = \{\mathbf{d}_{j_1}, \dots, \mathbf{d}_{j_n}\}$. We take the K

$$A = \left\{ \begin{array}{l} (-1, -1, 1) \\ (-2, -1, 3) \\ (1, -1, -3) \\ (1, 1, -2) \\ (2, 1, -1) \\ (1, 1, 1) \end{array} \right\}$$

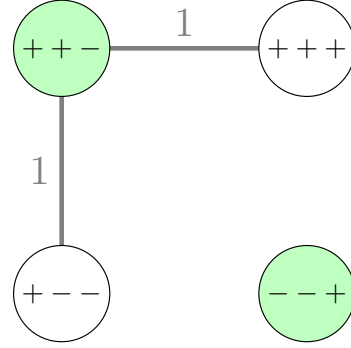
(a) The data set

$$\begin{array}{ll} (-1, -1, 1) & \mapsto \quad - - + \\ (-2, -1, 3) & \mapsto \quad - - + \\ (1, -1, -3) & \mapsto \quad + - - \\ (1, 1, -2) & \mapsto \quad + + - \\ (2, 1, -1) & \mapsto \quad + + - \\ (1, 1, 1) & \mapsto \quad + + + \end{array}$$

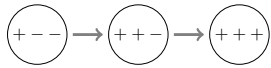
(b) Data points and corresponding sign labels.

$$V_0 = \left\{ \begin{array}{l} - - + \\ + - - \\ + + - \\ + + + \end{array} \right\}$$

(c) The set of sign labels V_0



(d) The graph G_0^1 . The set of proto-clusters W_0 is depicted in green.



(e) The walk obtained via BFS, assuming $\varphi_0 = + - -$.

$$\mathcal{C}_0 = \left\{ \left\{ + + -, + + + \right\} \right\}$$

(f) Suppose that the walk produces the collection \mathcal{C}_0 .

$$\mathcal{C}_1 = \left\{ \begin{array}{l} \{ + + -, + + + \} \\ \{ - - + \} \end{array} \right\}$$

(g) We form \mathcal{C}_1 by adding to \mathcal{C}_0 elements of W_0 not present in \mathcal{C}_0 .

$$\mathcal{C}_2 = \left\{ \left\{ \begin{array}{l} (1, 1, -2) \\ (2, 1, -1) \\ (1, 1, 1) \end{array} \right\}, \left\{ \begin{array}{l} (-1, -1, 1) \\ (-2, -1, 3) \end{array} \right\} \right\}$$

(h) The collection of clusters \mathcal{C}_2 , taking $k_0 = 2$.

Figure 5: Walk-through example illustrating the clustering process for a data set A with no rotation performed.

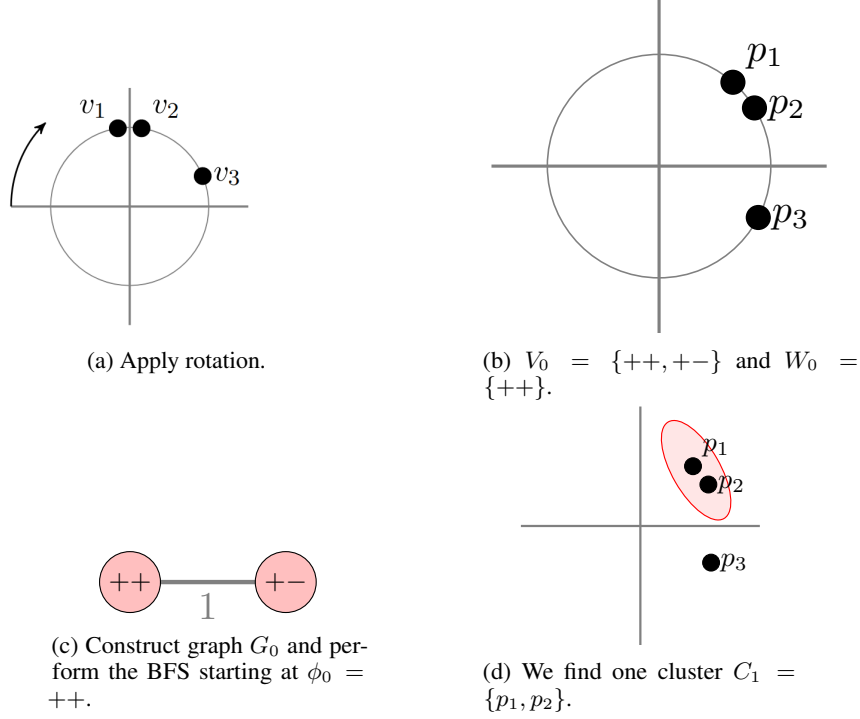


Figure 6: Walk-through example illustrating the effect of rotation: (a) A data set $A \subset \mathbb{S}^1 \subset \mathbb{R}^2$ given by the three points, to which an adequate rotation R is applied; (b) Corresponding sets V_0 and W_0 after rotation; (c) The graph G_0 and walk via BFS, using appropriate hyperparameters δ_0 and $k_0 > 1$; (d) Found cluster $C_2 = \{p_1, p_2\}$.

most frequent words in C^d , and denote this set of words by W_C^K . Finally, given a word w , we denote by \vec{w} a word embedding for w . The topic coherence of a cluster C is given by

$$\text{coh}(C) = \frac{\sum_{x,y \in W_C^K} \text{sim}(\vec{x}, \vec{y})}{\binom{K}{2}},$$

We define the topic coherence of the set of clusters \mathcal{C} as

$$\text{coh}(\mathcal{C}) = \frac{1}{|\mathcal{C}|} \sum_{C \in \mathcal{C}} \text{coh}(C).$$

Observe that $\text{coh}(\mathcal{C}) \in [-1, 1]$. The higher the value of $\text{coh}(\mathcal{C})$ is, the more coherent are the documents in each cluster, topic-wise.

2. Topic coherence using co-occurrences. This approach for evaluating a topic detection task is similar to the previous approach. However, instead of computing the semantic similarity between pair of topic words by means of the cosine similarity between their word embeddings, this approach computes their semantic similarity by counting co-occurrences using the pointwise mutual information [56].
3. Topic Majority. We consider the clustering task as a classification task, assigning a predicted topic to each cluster based on the majority topic among the topics of each document in the cluster. In this way, we have a topic prediction for each document that can be compared with its actual topic. We calculate and report the accuracy of this classification task (acc). We also report how many clusters have a majority topic out of the total number of clusters (m/t).
4. Adjusted Mutual Information. This is an information theoretic measure for clustering comparison quantifying the information shared by two clusters [57]. We use the implementation in `scikit-learn`. Here, it is worth pointing out that we are comparing both the baseline and our clustering method to the ground truth clustering, which might not be a clustering in the geometric sense. That is, documents sharing the same topic might not have vector representations close to each other. However, since we are comparing both clustering methods to the ground truth clustering, we report the results of this measure as a fair comparison score.

4 Experiments and Results

In this section we describe the experiments and results of the implementation of this clustering method in topic detection tasks using several text data sets. We compare this method with one of the most important density-based clustering methods, DBSCAN [1], in order to highlight its strengths and scope. In the next section we will interpret and discuss these results.

We use the following corpora of text documents:

- 20NewsGroups², which consists of 11000 documents. Each document in the corpus is marked with a single topic, there are 20 different topics.
- BBC Full Text Document Classification³, which consists of 2225 documents from the BBC news website corresponding to stories in five topical areas from 2004-2005. There are 5 different topics: business, entertainment, politics, sport, tech.
- Emotions data set for NLP⁴, which is a collection of 16000 short documents, each document has an emotion flag. This is a data set used mainly for sentiment analysis, however, we regard the emotion of each document as the topic of the document.

We used word and document embeddings with dimension $D = 100$ in the three corpora and the four embeddings models. Our experiments were conducted using standard computer equipment Intel Core i7@, 2.80GHz \times 8, and 16GB RAM.

We evaluate the clusters obtained using our method and DBSCAN using the four measures described in Section 3.3. The parameters for the clustering methods were chosen using a grid search, we use the parameters yielding the higher values of coh whenever the resulting clustering is not trivial.

In Tables 1 to 4, we report the scores of both clustering methods using the four measures.

Table 1: Coherence results, using the cosine similarity between word embeddings, for our clustering method compared to DBSCAN, in the three different corpora.

Topic coherence using the cosine similarity						
Model	20NG		BBC		Emotion	
	HOS-C	DBSCAN	HOS-C	DBSCAN	HOS-C	DBSCAN
word2vec	0.753	0.751	0.847	0.734	0.895	0.796
FastText	0.605	0.592	0.808	0.737	0.904	0.730
GloVe	0.422	0.260	0.392	0.256	0.295	0.198
doc2vec	0.397	0.491	0.512	0.581	0.917	0.796

Table 2: Coherence results, using pointwise mutual information between topic words, for our clustering method compared to DBSCAN, in the three different corpora.

Topic coherence using mutual information						
Model	20NG		BBC		Emotion	
	HOS-C	DBSCAN	HOS-C	DBSCAN	HOS-C	DBSCAN
word2vec	49.111	44.660	45.358	44.747	20.519	14.601
FastText	37.899	37.573	47.858	41.103	12.001	4.811
GloVe	36.132	72.123	42.860	50.481	17.268	17.085
doc2vec	36.029	72.495	34.049	41.349	22.502	26.065

5 Discussion

As we have previously set out, we evaluated and compared our clustering method using three types of measures. Firstly, we use coherence-based measures (Tables 1, 2), these measures account for how coherent are the most frequent words

²<http://qwone.com/~jason/20Newsgroups/>

³<https://www.kaggle.com/shivamkushwaha/bbc-full-text-document-classification>

⁴<https://www.kaggle.com/praveengovi/emotions-dataset-for-nlp>

Table 3: Accuracy results, using the topic majority classification, for our clustering method compared to DBSCAN, in the three different corpora.

Model	Accuracy											
	20NG				BBC				Emotion			
	HOS-C		DBSCAN		HOS-C		DBSCAN		HOS-C		DBSCAN	
	m/t	acc	m/t	acc	m/t	acc	m/t	acc	m/t	acc	m/t	acc
w2v	59/69	0.228	21/25	0.095	13/13	0.348	11/11	0.309	6/6	0.337	9/10	0.337
FT	59/75	0.263	31/34	0.137	6/6	0.405	18/20	0.325	3/3	0.336	14/15	0.339
GV	3/5	0.253	14/15	0.198	3/3	0.234	5/5	0.775	56/60	0.399	17/18	0.338
d2v	1/1	0.200	5/5	0.215	5/5	0.555	8/9	0.448	40/41	0.369	5/6	0.335

Table 4: Adjusted Mutual Information results, both our clustering method and DBSCAN are compared against the topic labels, in the three different corpora.

Model	Clustering adjusted mutual information					
	20NG		BBC		Emotion	
	HOS-C	DBSCAN	HOS-C	DBSCAN	HOS-C	DBSCAN
word2vec	0.166	0.024	0.111	0.047	0.004	0.001
FastText	0.123	0.036	0.135	0.062	0.001	0.001
GloVe	0.010	0.034	0.021	0.209	0.004	0.001
doc2vec	0.001	0.024	0.040	0.096	0.001	0.001

in the set of documents represented in each cluster. These measures do not take into account the original topics of the documents, instead they intrinsically evaluate the coherence of the topics in each cluster. Table 1 shows that our method performs better than DBSCAN. On the other hand, Table 2 shows that our method has a similar performance to DBSCAN.

Secondly, we measure the accuracy of the classification task (Table 3). As we can observe, our method performs better than DBSCAN. Lastly, we use adjusted mutual information, which is an information theoretic measure for clustering comparison (Table 4). As we have previously stated, we are comparing both clustering methods to the ground truth clustering, which might not be a good clustering in the geometric sense (we conjecture this from evidence depicted in Figure 7). As a consequence of this, the values of Table 4 are low for both methods. This evidence shows that both methods have similar performances when evaluated with this measure. Other information theoretic measure, such as mutual information and adjusted rank index, exhibited similar scores.

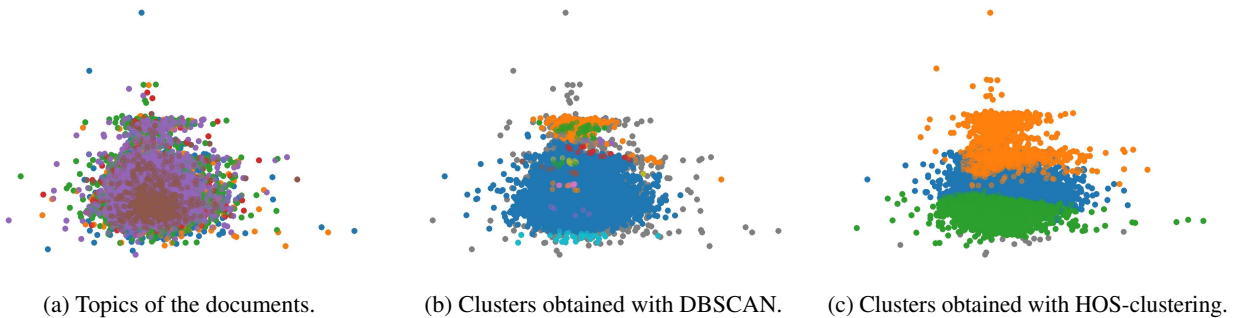


Figure 7: Dimensionality reduction, using PCA, after clustering of the Emotion data set with FastText embeddings. Although the actual behaviour of the points in \mathbb{R}^D may be different, it is very likely that there is a high overlap between the different topics, which makes clustering difficult.

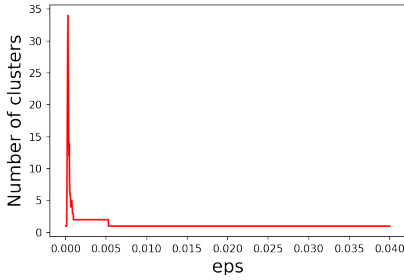
As a side remark, it is worth noting that both clustering methods performed systematically worse on the data sets consisting of GloVe word embeddings. Although there are techniques aiming to normalize the values of entropy-based measures for clustering comparison, so that they show comparable values across different data sets [58], we decided to keep the original values to show this interesting phenomenon. We will study this phenomenon in future work to shed

some light into the difference of the four word embeddings models when capturing semantic regularities regarding topic detection.

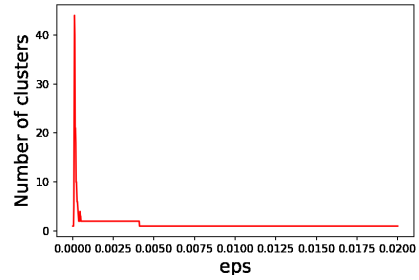
Taking into account all evaluation metrics on both clustering methods, we conclude that our clustering method allows to generate text clusters having a quality similar to the state of the art. However, our method shows advantages and differences over DBSCAN, which we now enumerate.

DBSCAN strongly depends on the hyper parameter ϵ , which accounts for the maximum distance between two samples, for one to be considered in the vicinity of the other. Appropriately choosing this parameter is not a trivial task. Some heuristics for choosing this parameter have been discussed in the literature [45]. However, we found that in this high-dimensional case, a small variation of ϵ produces large variations in the number of clusters, and overall in the clustering results. Moreover, the range of ϵ values that give non-trivial clustering results is very narrow. Examples of this are shown in Figures 8a and 8b.

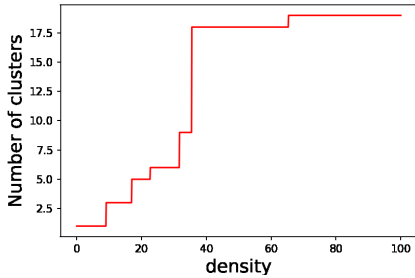
In contrast, our evidence suggests that our method is more stable under variations of the main hyper-parameter δ_0 . If δ_0 is small, all points in hyperoctants represented by the nodes of the graph $G_{\sigma_0}^{d_0}$ will form one cluster. On the other hand, if δ_0 is large, we will have as many clusters as *proto-clusters* $P \in W_0$ satisfying that $P > k_0$. This number is the maximum *resolution* of our method. This simplifies the task of fine tuning the method in order to produce better results, since the interval of values of δ_0 yielding non-trivial clustering results has infinite length. This behaviour is depicted in Figures 8c, 8d. This previously described scenario explains why our method is only able to find at most 18 clusters in 8c, and 5 in 8d.



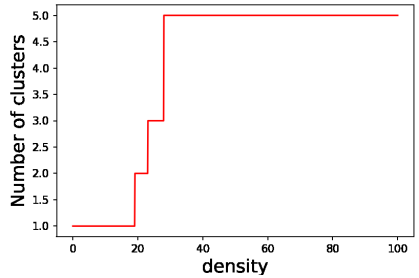
(a) DBSCAN applied to the word2vec embeddings of the BBC data set.



(b) DBSCAN applied to the FastText embeddings of the Emotion data set.



(c) HOS-Clustering applied to the word2vec embeddings of the BBC data set.

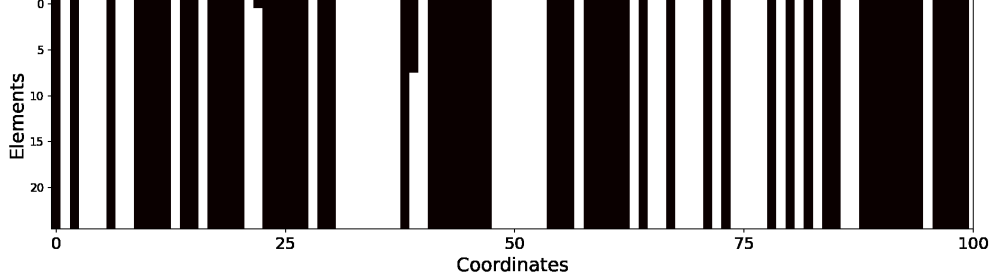


(d) HOS-Clustering applied to the FastText embeddings of the BBC data set.

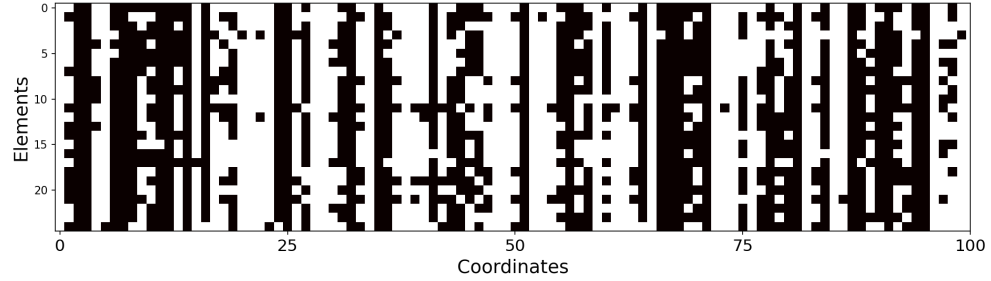
Figure 8: Number of clusters found by DBSCAN as a function of the hyperparameter ϵ (top); and number of clusters found by HOS-Clustering as a function of the hyperparameter δ_0 (bottom).

Finally, but not the least, it is worth noting that our method is not only a clustering method, but also a tool for exploring the data set from a topological perspective. The reduction in the size of the set of entities when we go from A to V_0 gives information about how concentrated are the points in the space. In other words, we know in how many regions the data set is located. For example, in the BBC corpus, using the FastText embeddings, after the appropriate rotation, there are only 16 hyperoctants containing the 2225 points. On the other hand, using the GloVe embeddings, there are 2070 hyperoctants containing the 2225 points. This difference immediately indicates that GloVe embeddings are more sparsely distributed in space than FastText embeddings.

For illustrative purposes of the effects of clustering under our approach, in Figure 9 we show the difference in sign vectors between a cluster of points (Figure 9a, and a random set of points (Figure 9b). Each plot represents a set A of n d -dimensional vectors as a heatmap of a $n \times d$ matrix with entries $\{-1, 1\}$. Each row is the sign vector of a vector of A . In this case, $n = 30$, $d = 100$. Both sets are subsets of the FastText documents embeddings of the Emotion data set. The difference between these two graphs provides insight into clustering using hyperoctants. As we observe, in the cluster depicted in Figure 9a there are only points in three different hyperoctants.



(a) Signs of the coordinates of each document embedding in a cluster.



(b) Signs of the coordinates of each document embedding in a random set of embeddings.

Figure 9: Two different sets of 25 document FastText embeddings in the Emotion corpus. Each plot is a rectangular 25×100 grid, where each row represents the signs of the 100 coordinates of the embedding (+:black; -: white) : a) A set of embeddings displaying only three different combinations of signs in their coordinates, thus evidencing the fact that these 25 embeddings forms one cluster; b) A set of embeddings displaying many different different combinations of signs in their coordinates, thus evidencing the fact that they do not form any cluster.

Now, we discuss the weaknesses of our method. Consider the following scenario in a data set A , there are two subsets $C_1, C_2 \subset A$ which are ground truth clusters, such that $\text{diam}(C_1 \cup C_2) < \frac{\pi}{2}$. In other words, we have two ground truth clusters that, after an appropriate rotation, lie in the same hyperoctant. In this scenario, our method will join the points in $C_1 \cup C_2$ in only one cluster. However, as we discussed in Observation 1, as the dimension increases, the probability of such a situation occurring decreases exponentially, and the fact that two points are in the same hyperoctant becomes more meaningful in terms of clustering. In future work, we will address this limitation by properly embedding such hyperoctants in a higher dimensional space.

Moreover, as we have described, our method is suitable for data sets in spaces endowed with the angular metric, which could be seen as a limitation. However, if an Euclidean D -space is properly embedded in a D -dimensional \mathbb{R}^{D+1} -sphere, it is possible to apply our clustering method to this embedded data set. This will be described in a future paper.

Regarding the question of how big should be the dimension D of the feature space in order to use our method, it should satisfy

$$D > \frac{\log N}{\log 2} \tag{7}$$

where N is the number of points in the data set. This guarantees that there is enough hyperoctants to contain each point of the data set. Thus, giving significance to the fact that two points lie in the same hyperoctant. If condition (7) does not hold, at least two points are bound to lie in the same hyperoctant, not because they are necessarily close to each other, but because of the pigeonhole principle. Addressing the behaviour of this method in even higher dimensions, we

would like to mention here that we conducted experiments with these corpora using BERT’s vector representations (with dimension 512), but they were not reported because the coherence metrics, used for the exhaustive comparison, are not adapted to the properties of these embeddings. This will be part of future work.

As a last point of this section, we would like to briefly discuss the connections our clustering method has with other research fields. A first aspect is the connections that the graph of hyperoctants P_D suggests. P_D can be regarded as the Hasse diagram of the power-set lattice $P_{\text{fin}}(\phi(A))$ [59]. It is also isomorphic to the binary Hamming space, which is the set of all 2^N binary strings of length N , used in the theory of signals coding and transmission [60].

Furthermore, there are other possible applications and connections of our approach to code theory. Using the language of this research realm [61], and our notation, we rotate our original data set A , thus obtaining the data set V_0 which will be clustered. This rotated data set is a (D, N, α) code of length N in the space \mathbb{F}_2^D . This code has certain minimum distance $\alpha \in [0, D]$, and some covering radius $r \in [0, D]$. Here, \mathbb{F}_2 denotes the finite field of two elements. This code is not necessarily linear.

To briefly illustrate our point, we explore two concepts of code theory, applied to our setting. Firstly, we explore the covering radius r . A r -covering binary code is a finite subset $V \subset \mathbb{F}_2^D$ such that, for every code-word $y \in \mathbb{F}_2^D$, there exist $x \in V$ such that $d_L(x, y) \leq r$. In other words, the union of all closed balls of radius r around code-words of V cover the space \mathbb{F}_2^D . The covering radius of the code V is the smallest r such that V is r -covering. Covering codes is a central object in coding theory, they have found applications in diverse areas. Generally, one is interested in the estimation of $K(D, r)$, the minimum cardinality of a binary code of length D and covering radius r . For a data set V_0 , the bigger the covering radius, the more evenly distributed are the points in the different hyperoctants, and thus, the least discernible are the possible clusters. A clear cluster should be a r -covering sub-code $B \subset V_0$ with a large r . Thus, the clustering method translates into finding different subsets $C \subset V_0$ such that every one of these sets C is a r -covering code with a large r depending on the value of δ_0 . In this setting, given a minimum density δ_0 , we can estimate d_0 , and therefore, $K(D, d_0)$ gives a lower bound for the number of instances necessary for obtaining a non-trivial clustering. On the other hand, linearity imposes strong restrictions on V_0 , and ultimately, on the possible coordinates of the points of the data set. For example, for every two code-words $x, y \in V_0$, it should hold $x + y \in V_0$. Linear codes exhibit regularities in \mathbb{F}_2^D , which a general data set might not satisfy. Therefore, in the setting of this method, we are interested in non-linear codes.

These previous arguments show the potential interplay between our clustering method and code theory. These ideas will be developed in a future paper.

A last word on the applications of the proposed method is worth mentioning. Our method could also be useful in the analysis of high-dimensional data such as images or genomic sequences [62]. Finally, since there are many contributions using the Hamming and Levenshtein distances, or sign matrices, our method could have an impact on other realms of research such as bioinformatics [63, 62, 64], pattern recognition [65], image retrieval [66], data mining [67], communication complexity and learning theory [68].

6 Conclusions

Clustering is part of the exploratory data methods that aim at enhancing the practitioner’s natural ability to recognize patterns in the data being studied.

In this work, we proposed a new clustering method called Hyperoctant-Search Clustering, based on a combinatorial-topological approach applied to regions of space defined by signs of coordinates (hyperoctants). The method builds clusters of data points based on the partitioning of a connected graph, whose vertices represent hyperoctants, and whose edges connect neighboring hyperoctants under the Levenshtein distance.

Clustering has many useful applications. As our method is best suited for high-dimensional spaces, where data points contain positive and negative features—typical examples of which are dense vector representations (embeddings) produced by neural networks—in this paper we selected topic detection to assess the performance of the proposed method. Our objective was to explore, via clustering, the similarities between dense vector representations of documents, in order to discover semantic relationships possibly encoded by patterns of signs in the embeddings.

Our experimental results provide evidence that our method is a sound alternative to perform clustering tasks in high-dimensional spaces endowed with the angular metric, allowing also to acquire insight about some topological properties of the semantic space, and having a stable performance under variations of its most important hyperparameter.

The ability provided by the proposed method to explore data from a topological perspective extends the current possibilities of exploring high-dimensional data. As our experiments show, the method helps to gain insight into the distribution of the embeddings in the semantic space, pinpointing both void and highly populated regions, as it directly

provides information on the number of hyperoctants where there are data points. The smaller this number is compared to the total number of points, the more “irregular” the distribution of the set of points in space is. In this sense, our method works better the more “irregularities” there are in the distribution of the set of points in space; that is, the more clusterable the input problem is. This phenomenon, intrinsic to the clustering problem, has already been extensively discussed in the past, where it has been observed that if the problem is not clusterable from the start, no method will be able to solve it. As [50] have eloquently set out: “*if a data set is hard to cluster then it does not have a meaningful clustering structure*”, [...] *the hard cases that render clustering NP-hard are the inputs we don’t care to cluster*[50, p. 1]. An in-depth study of this topological data analysis capability of our method will be part of future work.

Acknowledgments

The authors acknowledge the support of CONAHCYT (now SECIHTI).

References

- [1] Martin Ester, Hans-Peter Kriegel, Jörg Sander, and Xiaowei Xu. A density-based algorithm for discovering clusters in large spatial databases with noise. In *Proceedings of the Second International Conference on Knowledge Discovery and Data Mining, KDD’96*, page 226–231, Portland, Oregon, 1996. AAAI Press.
- [2] Mihael Ankerst, Markus M. Breunig, Hans-Peter Kriegel, and Jörg Sander. Optics: Ordering points to identify the clustering structure. In *Proceedings of the 1999 ACM SIGMOD International Conference on Management of Data, SIGMOD ’99*, page 49–60, New York, NY, USA, 1999. Association for Computing Machinery.
- [3] Anil K. Jain and Richard C. Dubes. *Algorithms for Clustering Data*. Prentice-Hall, Inc., USA, 1988.
- [4] Michael Steinbach, Levent Ertöz, and Vipin Kumar. *The Challenges of Clustering High Dimensional Data*, pages 273–309. Springer Berlin Heidelberg, 2004.
- [5] Nicholas Monath, Kumar Avinava Dubey, Guru Guruganesh, Manzil Zaheer, Amr Ahmed, Andrew McCallum, Gokhan Mergen, Marc Najork, Mert Terzihan, Bryon Tjanaka, Yuan Wang, and Yuchen Wu. Scalable hierarchical agglomerative clustering. In *Proceedings of the 27th ACM SIGKDD Conference on Knowledge Discovery & Data Mining, KDD ’21*, page 1245–1255, New York, NY, USA, 2021. Association for Computing Machinery.
- [6] Yong Shi, Zhensong Chen, Zhiquan Qi, Fan Meng, and Limeng Cui. A novel clustering-based image segmentation via density peaks algorithm with mid-level feature. *Neural Computing and Applications*, 28(1):29–39, 2017.
- [7] Tarun Yellamraju and Mireille Boutin. Clusterability and clustering of images and other “real” high-dimensional data. *IEEE Transactions on Image Processing*, 27(4):1927–1938, 2018.
- [8] D Sailaja, M Kishore, B Jyothi, and NRGK Prasad. An overview of pre-processing text clustering methods. *Int. J. Comput. Sci. Inform. Tech*, 6:3119–24, 2015.
- [9] Yutong Li, Juanjuan Cai, and Jingling Wang. A text document clustering method based on weighted bert model. In *2020 IEEE 4th Information Technology, Networking, Electronic and Automation Control Conference (ITNEC)*, volume 1, pages 1426–1430. IEEE, 2020.
- [10] Vivek Mehta, Seema Bawa, and Jasmeet Singh. Weclustering: word embeddings based text clustering technique for large datasets. *Complex & Intelligent Systems*, 7(6):3211–3224, 2021.
- [11] Yoshua Bengio, Réjean Ducharme, Pascal Vincent, and Christian Jauvin. A neural probabilistic language model. *Journal of machine learning research*, 3(Feb):1137–1155, 2003.
- [12] Tomas Mikolov, Ilya Sutskever, Kai Chen, Greg S Corrado, and Jeff Dean. Distributed representations of words and phrases and their compositionality. In *Advances in neural information processing systems*, pages 3111–3119, 2013.
- [13] Jeffrey Pennington, Richard Socher, and Christopher Manning. GloVe: Global vectors for word representation. In *Proceedings of the 2014 Conference on Empirical Methods in Natural Language Processing (EMNLP)*, pages 1532–1543, Doha, Qatar, October 2014. Association for Computational Linguistics.
- [14] Ashish Vaswani, Noam Shazeer, Niki Parmar, Jakob Uszkoreit, Llion Jones, Aidan N Gomez, Łukasz Kaiser, and Illia Polosukhin. Attention is all you need. In I. Guyon, U. V. Luxburg, S. Bengio, H. Wallach, R. Fergus, S. Vishwanathan, and R. Garnett, editors, *Advances in Neural Information Processing Systems*, volume 30, pages 1–11, Long Beach Convention Center, Long Beach, 2017. Curran Associates, Inc.
- [15] Jacob Devlin, Ming-Wei Chang, Kenton Lee, and Kristina Toutanova. BERT: Pre-training of deep bidirectional transformers for language understanding. In *Proceedings of the 2019 Conference of the North American Chapter of the Association for Computational Linguistics: Human Language Technologies, Volume 1 (Long and Short Papers)*, pages 4171–4186, Minneapolis, Minnesota, June 2019. Association for Computational Linguistics.

- [16] Zhuosheng Zhang, Yuwei Wu, Hai Zhao, Zuchao Li, Shuailiang Zhang, Xi Zhou, and Xiang Zhou. Semantics-aware bert for language understanding. In *Proceedings of the AAAI Conference on Artificial Intelligence*, volume 34, pages 9628–9635, 2020.
- [17] Anna Rogers, Olga Kovaleva, and Anna Rumshisky. A primer in BERTology: What we know about how BERT works. *Transactions of the Association for Computational Linguistics*, 8:842–866, 2020.
- [18] James V Haxby, Andrew C Connolly, and J Swaroop Guntupalli. Decoding neural representational spaces using multivariate pattern analysis. *Annual review of neuroscience*, 37:435–456, 2014.
- [19] Jona Sassenhagen and Christian J Fiebach. Traces of meaning itself: Encoding distributional word vectors in brain activity. *Neurobiology of Language*, 1(1):54–76, 2020.
- [20] Jingcheng Du, Peilin Jia, Yulin Dai, Cui Tao, Zhongming Zhao, and Degui Zhi. Gene2vec: distributed representation of genes based on co-expression. *BMC genomics*, 20(1):7–15, 2019.
- [21] Hans-Friedrich Köhn and Lawrence J Hubert. Hierarchical cluster analysis. *Wiley StatsRef: Statistics Reference Online*, pages 1–13, 2014.
- [22] J. MacQueen. Some methods for classification and analysis of multivariate observations. In *Proceedings of the Fifth Berkeley Symposium on Mathematical Statistics and Probability, Volume 1: Statistics*, pages 281–297, Berkeley, Calif., 1967. University of California Press.
- [23] Inderjit S Dhillon and Dharmendra S Modha. Concept decompositions for large sparse text data using clustering. *Machine learning*, 42(1-2):143–175, 2001.
- [24] Volkan Tunali, Turgay Bilgin, and Ali Camurcu. An improved clustering algorithm for text mining: Multi-cluster spherical k-means. *International Arab Journal of Information Technology (IAJIT)*, 13(1), 2016.
- [25] Šárka Brodinová, Peter Filzmoser, Thomas Ortner, Christian Breiteneder, and Maia Rohm. Robust and sparse k-means clustering for high-dimensional data. *Advances in Data Analysis and Classification*, 13(4):905–932, 2019.
- [26] Evelyn Fix and Joseph Lawson Hodges. Discriminatory analysis. nonparametric discrimination: Consistency properties. *International Statistical Review/Revue Internationale de Statistique*, 57(3):238–247, 1989.
- [27] Jie Chen, Haw-ren Fang, and Yousef Saad. Fast approximate knn graph construction for high dimensional data via recursive lanczos bisection. *J. Mach. Learn. Res.*, 10:1989–2012, dec 2009.
- [28] Wei Zhang, Xiaogang Wang, Deli Zhao, and Xiaoou Tang. Graph degree linkage: Agglomerative clustering on a directed graph. In *European Conference on Computer Vision*, pages 428–441. Springer, 2012.
- [29] Wen Li, Ying Zhang, Yifang Sun, Wei Wang, Mingjie Li, Wenjie Zhang, and Xuemin Lin. Approximate nearest neighbor search on high dimensional data—experiments, analyses, and improvement. *IEEE Transactions on Knowledge and Data Engineering*, 32(8):1475–1488, 2019.
- [30] Levent Ertöz, Michael Steinbach, and Vipin Kumar. Finding clusters of different sizes, shapes, and densities in noisy, high dimensional data. In *Proceedings of the 2003 SIAM international conference on data mining*, pages 47–58. SIAM, 2003.
- [31] Panthadeep Bhattacharjee and Pinaki Mitra. A survey of density based clustering algorithms. *Frontiers of Computer Science*, 15(1):1–27, 2021.
- [32] Kevin S. Beyer, Jonathan Goldstein, Raghu Ramakrishnan, and Uri Shaft. When is "nearest neighbor" meaningful? In *Proceedings of the 7th International Conference on Database Theory, ICDT '99*, page 217–235, Berlin, Heidelberg, 1999. Springer-Verlag.
- [33] Charles Bouveyron, Stéphane Girard, and Cordelia Schmid. High-dimensional data clustering. *Computational statistics & data analysis*, 52(1):502–519, 2007.
- [34] Yunchao Gong, Marcin Pawlowski, Fei Yang, Louis Brandy, Lubomir Bourdev, and Rob Fergus. Web scale photo hash clustering on a single machine. In *Proceedings of the IEEE conference on computer vision and pattern recognition*, pages 19–27, 2015.
- [35] Jingdong Wang, Ting Zhang, Nicu Sebe, Heng Tao Shen, et al. A survey on learning to hash. *IEEE transactions on pattern analysis and machine intelligence*, 40(4):769–790, 2017.
- [36] Fumin Shen, Yang Yang, Li Liu, Wei Liu, Dacheng Tao, and Heng Tao Shen. Asymmetric binary coding for image search. *IEEE Transactions on Multimedia*, 19(9):2022–2032, 2017.
- [37] Zheng Zhang, Li Liu, Fumin Shen, Heng Tao Shen, and Ling Shao. Binary multi-view clustering. *IEEE transactions on pattern analysis and machine intelligence*, 41(7):1774–1782, 2018.

- [38] Xiaobo Shen, Weiwei Liu, Ivor Tsang, Fumin Shen, and Quan-Sen Sun. Compressed k-means for large-scale clustering. In *Thirty-first AAAI conference on artificial intelligence*, 2017.
- [39] Bin Fan, Qingqun Kong, Baoqian Zhang, Hongmin Liu, Chunhong Pan, and Jiwen Lu. Efficient nearest neighbor search in high dimensional hamming space. *Pattern Recognition*, 99:107082, 2020.
- [40] Rakesh Agrawal, Johannes Gehrke, Dimitrios Gunopulos, and Prabhakar Raghavan. Automatic subspace clustering of high dimensional data for data mining applications. In *Proceedings of the 1998 ACM SIGMOD international conference on Management of data*, pages 94–105, 1998.
- [41] Chun-Hung Cheng, Ada Waichee Fu, and Yi Zhang. Entropy-based subspace clustering for mining numerical data. In *Proceedings of the fifth ACM SIGKDD international conference on Knowledge discovery and data mining*, pages 84–93, 1999.
- [42] Xuyang Yan, Shabnam Nazmi, Berat A Erol, Abdollah Homaifar, Biniam Gebru, and Edward Tunstel. An efficient unsupervised feature selection procedure through feature clustering. *Pattern Recognition Letters*, 131:277–284, 2020.
- [43] Huazhu Chen, Weiwei Wang, and Shousheng Luo. Coupled block diagonal regularization for multi-view subspace clustering. *Data Mining and Knowledge Discovery*, July 2022.
- [44] Hans-Peter Kriegel, Peer Kröger, and Arthur Zimek. Clustering high-dimensional data: A survey on subspace clustering, pattern-based clustering, and correlation clustering. *ACM Trans. Knowl. Discov. Data*, 3(1), march 2009.
- [45] Erich Schubert, Jörg Sander, Martin Ester, Hans Peter Kriegel, and Xiaowei Xu. Dbscan revisited, revisiteschubert2017dbscand: why and how you should (still) use dbscan. *ACM Transactions on Database Systems (TODS)*, 42(3):1–21, 2017.
- [46] Rui Xu and Donald Wunsch. Survey of clustering algorithms. *IEEE Transactions on neural networks*, 16(3):645–678, 2005.
- [47] Tianyi Huang, Shiping Wang, and William Zhu. An adaptive kernelized rank-order distance for clustering non-spherical data with high noise. *International Journal of Machine Learning and Cybernetics*, 11(8):1735–1747, August 2020.
- [48] Leszek Gasieniec, Jesper Jansson, and Andrzej Lingas. Approximation algorithms for Hamming clustering problems. *Journal of Discrete Algorithms*, 2(2):289–301, 2004.
- [49] Marina Meilă. Local equivalences of distances between clusterings—a geometric perspective. *Machine Learning*, 86(3):369–389, March 2012.
- [50] Margareta Ackerman and Shai Ben-David. Clusterability: A theoretical study. In David van Dyk and Max Welling, editors, *Proceedings of the Twelfth International Conference on Artificial Intelligence and Statistics*, volume 5 of *Proceedings of Machine Learning Research*, pages 1–8, Hilton Clearwater Beach Resort, Clearwater Beach, Florida USA, 16–18 Apr 2009. PMLR.
- [51] Jon Kleinberg. An impossibility theorem for clustering. In S. Becker, S. Thrun, and K. Obermayer, editors, *Advances in Neural Information Processing Systems*, volume 15, page 463–470, Cambridge, MA, USA, 2002. MIT Press.
- [52] Vladimir I Levenshtein. Binary codes capable of correcting deletions, insertions, and reversals. In *Soviet physics doklady*, volume 10, pages 707–710, 1966. Number: 8.
- [53] Tomas Mikolov, Kai Chen, Greg Corrado, and Jeffrey Dean. Efficient estimation of word representations in vector space. *arXiv preprint arXiv:1301.3781*, 2013.
- [54] Piotr Bojanowski, Edouard Grave, Armand Joulin, and Tomas Mikolov. Enriching word vectors with subword information. *arXiv preprint arXiv:1607.04606*, 2016.
- [55] David Newman, Jey Han Lau, Karl Grieser, and Timothy Baldwin. Automatic evaluation of topic coherence. In *Human language technologies: The 2010 annual conference of the North American chapter of the association for computational linguistics*, pages 100–108, 2010.
- [56] Aminul Islam and Diana Inkpen. Second order co-occurrence pmi for determining the semantic similarity of words. In *Proceedings of the Fifth International Conference on Language Resources and Evaluation (LREC’06)*, 2006.
- [57] Nguyen Xuan Vinh, Julien Epps, and James Bailey. Information theoretic measures for clusterings comparison: Variants, properties, normalization and correction for chance. *The Journal of Machine Learning Research*, 11:2837–2854, 2010.

- [58] Ping Luo, Hui Xiong, Guoxing Zhan, Junjie Wu, and Zhongzhi Shi. Information-theoretic distance measures for clustering validation: Generalization and normalization. *IEEE Transactions on Knowledge and Data Engineering*, 21(9):1249–1262, 2008.
- [59] Brian A Davey and Hilary A Priestley. *Introduction to lattices and order*. Cambridge university press, United Kingdom, 2002.
- [60] John Baylis. *Error-correcting codes: a mathematical introduction*. Routledge, Abingdon, UK, 2018.
- [61] J.H. van Lint. *Coding theory*, pages 773–807. Elsevier, 1995.
- [62] David S Campo and Yury Khudyakov. Convex hulls in hamming space enable efficient search for similarity and clustering of genomic sequences. *BMC bioinformatics*, 21(18):1–13, 2020.
- [63] Robert Logan, Zoe Fleischmann, Sofia Annis, Amy Wangsness Wehe, Jonathan L. Tilly, Dori C. Woods, and Konstantin Khrapko. 3GOLD: optimized Levenshtein distance for clustering third-generation sequencing data. *BMC Bioinformatics*, 23(1):95, March 2022.
- [64] Charlotte Wang, Wen-Hsin Kao, and Chuhsing Kate Hsiao. Using Hamming Distance as Information for SNP-Sets Clustering and Testing in Disease Association Studies. *PLOS ONE*, 10(8):1–24, August 2015. Publisher: Public Library of Science.
- [65] Bin Fan, Qingqun Kong, Baoqian Zhang, Hongmin Liu, Chunhong Pan, and Jiwen Lu. Efficient nearest neighbor search in high dimensional hamming space. *Pattern Recognition*, 99:107082, 2020.
- [66] Sana Fakhfakh, Mohamed Tmar, and Walid Mahdi. Image Retrieval Based on Using Hamming Distance. *Procedia Computer Science*, 73:320–327, January 2015.
- [67] Peng Zhang, Xiaogang Wang, and Peter X.-K Song. Clustering categorical data based on distance vectors. *Journal of the American Statistical Association*, 101(473):355–367, 2006.
- [68] Satyanarayana V Lokam et al. Complexity lower bounds using linear algebra. *Foundations and Trends® in Theoretical Computer Science*, 4(1–2):1–155, 2009.